

# Direct Measurement of the impulse in a Magnetic Thrust Chamber System for Laser Fusion Rocket

Akihiro Maeno,\* Naoji Yamamoto, and Hideki Nakashima  
*Interdisciplinary Graduate School of Engineering Science,  
Kyushu University, 6-1 Kasuga-kouen, Kasuga, Fukuoka 816-8580, Japan*

Shinsuke Fujioka and Tomoyuki Johzaki  
*Institute of Laser Engineering, Osaka University, Suita, Osaka 565-087, Japan*

Yoshitaka Mori  
*The Graduate School for the Creation of New Photonics Industries, Hamamatsu, Shizuoka 431-1202, Japan*

Atsushi Sunahara  
*Institute for Laser Technology, Suita, Osaka 565-087, Japan*  
(Dated: May 31, 2011)

An experiment is conducted to measure an impulse for demonstrating a magnetic thrust chamber system for laser fusion rocket. The impulse is produced by the interaction between plasma and magnetic field. In the experiment, the system consists of plasma and neodymium permanent magnets. The plasma is created by a single-beam laser aiming at a polystyrene spherical target. The impulse is 1.5 to 2.2  $\mu\text{Ns}$  by means of a pendulum thrust stand, when the laser energy is 0.7 J. Without magnetic field, the measured impulse is found to be zero. These results indicate that the system for generating impulse is working.

In the future, a space propulsion system providing large thrust with high specific impulse (proportional to the exhaust velocity) will be necessary for manned space flight to Mars. One promising candidate for such a system is Laser Fusion Rocket [1–4] (LFR) proposed in the 1970s by Hyde [1, 2]. Here, the propulsion system to produce thrust is called as “magnetic thrust chamber system”. The system produces an impulse (momentum per pulse) by using diamagnetic current in plasma. Fig. 1 shows the mechanism of producing an impulse in the system as follows.

- (a) An inertial confinement fusion (ICF) reaction can release a large amount of energy, and create a high temperature and high density plasma. The resulting fusion plasma expands in properly designed applied magnetic field geometry. For the magnetic thrust chamber system for LFR, the magnetic field geometry is typically produced by a solenoid superconducting magnet (SCM).
- (b) Since plasma is a good conductor, when a magnetic field is applied, charged particles begin Larmor motion. The Larmor motion induces diamagnetic current sweeping aside the magnetic field. As a result, the magnetic field is compressed by the diamagnetic current.
- (c) The compressed magnetic field pushes back the plasma, similar to a spring that oscillates. As a result, the LFR system produces an impulse by

the interaction between the diamagnetic current in the plasma and the magnetic field provided by the SCM.

The advantages [5, 6] of the LFR system are as follows. First, short duration space mission is possible for LFR owing to its large thrust and high specific impulse. This can reduce the exposure of a space vehicle crew to cosmic radiations; the exposure is the greatest problem for manned space flight. Second, the thrust of the system can be flexibly varied in the mission by varying laser pulse repetition rate, plasma and magnetic field conditions. This characteristic allows for flexible acceleration of the vehicle that will be necessary in many missions. Third, LFR has a long lifetime. The plasma does not directly interact with the solid wall of the vehicle since the plasma can be controlled by the magnetic field, no damage to the vehicle structure occurs and little plasma energy is wasted, which leads to long lifetime.

Several studies have been conducted to investigate various plasma behaviors for producing an impulse. They focused on Rayleigh-Taylor (RT) instability and electrons detachment from magnetic field. Since RT instability would lead to impulse reduction, Nagamine *et al.* [7] found that RT instability would not be serious problems for the system by using a three-dimensional (3D) hybrid particle-in-cell (PIC) code. When electrons would not detach from the magnetic field, ions would be pulled back to the space vehicle by a charge-separation electric field generated by ion and electron motions. As a result, a space vehicle cannot get enough thrust. Kawabuchi *et al.* [8] found that electrons detachment would occur by using a two-dimensional in coordinate space and 3D in velocity space electromagnetic full PIC code. Vchivokv

---

\* maeno@aees.kyushu-u.ac.jp



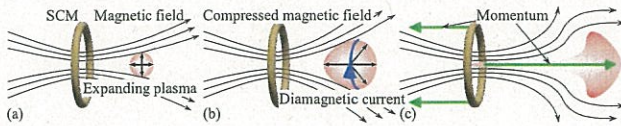


FIG. 1. Mechanism of producing an impulse in magnetic thrust chamber system for LFR. (a) Expanding ICF plasma in a properly designed applied magnetic field geometry. (b) Compressed magnetic field and diamagnetic current induced by Larmor motion. (c) Compressed magnetic field pushing back the plasma.

*et al.* [9] observed temporal plasma behaviors in an axially symmetric dipole magnetic field, the magnetic thrust chamber system for LFR. They estimated the impulse and observed the diamagnetic cavity in their magnetic probe experiments. The diamagnetic cavity was formed against the applied magnetic field. These results indicate that the impulse is produced on the system.

A direct measurement of the impulse produced by the interaction between plasma and magnetic field has not yet been performed. The present paper is the first report that attempts to measure the impulse directly. In this paper, an experiment to demonstrate the magnetic thrust chamber system for LFR is conducted by using laser-produced plasma and neodymium permanent magnets in place of ICF plasma and SCM.

The experiments are conducted to measure the impulse by means of a pendulum thrust stand, as shown in Fig. 2. Laser-produced plasma is created by a 1064 nm single-beam Nd:YAG laser focusing into a 500  $\mu\text{m}$  wide in diameter polystyrene spherical target. The laser spot diameter is the same as the target diameter by using a lens having F-number of 20. The target is suspended at the end by carbon fiber with a glass stick to decrease the measurement error caused by the ablation plasma of the glass stick. Six cylindrical neodymium permanent magnets connected in the axial direction are used for producing the magnetic field. The surface magnetic flux density of each individual permanent magnet is 0.47 T. The magnet itself is 16 mm in diameter and 10 mm long. The permanent magnets are arranged so as not to disturb the incoming laser beam. In particular, the distance between the surface of the permanent magnets and the target center is 11 mm, and the angle between the axis of permanent magnets and the laser beam is 45 degrees. The magnetic field strength of the axis at the target is calculated to be 0.12 T, as shown in Fig. 2.

The pendulum thrust stand [10, 11] in this experiment (see Fig. 3) is composed of the permanent magnets, knife edges, counter weights, Light Emitting Diode (LED) displacement sensors, and an oil damper. These magnets are installed on the top of the pendulum. The pendulum is supported by the knife edges mounted on side posts. The counter weight is placed on the pendulum to create a vertical balance such that the center of gravity is around the pendulum's axis of rotation. In this fashion, the pendulum swings easily even for a small impulse. The

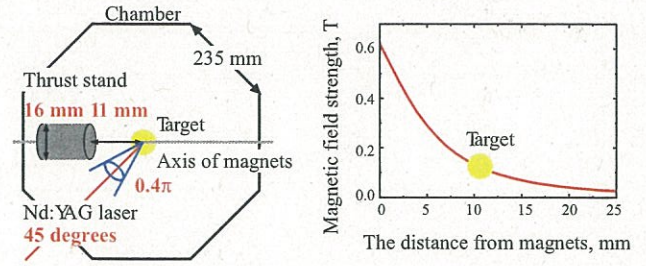


FIG. 2. Experimental setup and the calculated magnetic field strength along the axis of the permanent magnets as a function of the distance from the surface of the permanent magnets.

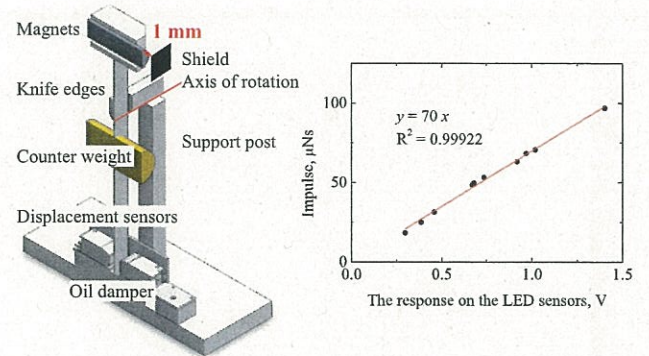


FIG. 3. Schematic of the shielded thrust stand (vertical sectional view) and applied calibration force as a function of the signals of LED sensors and the liner curve fitting to the calibration data.

natural period of this pendulum is about 1.2 second. The deflection of the pendulum is detected by the LED displacement sensors. To decrease the error in the impulse measurement, i.e., to offset the mechanical noise experienced by the sensors, the LED sensors are placed face-to-face and supplied by a single power source. The oil damper is installed to suppress mechanical noise induced by background vibrations, which are critical problems for small impulse measurements. To remove the momentum induced by direct collision between the expanding plasma and permanent magnets, a plate is placed at a distance of 1 mm from the magnets to shield from the plasma. This plate is connected to a grounded vacuum chamber. In this paper, this thrust stand is called as "shielded" thrust stand.

Calibration of the thrust stand is performed by striking the thrust stand with an impact which is measured directly by a force transducer attached to the counter weight. The force transducer records the history of the impulsive force, whose integral yields the impulse of the strike. The impulse on the force transducer is proportional to the amplitude on the LED displacement sensors converted from the deflection of the pendulum [10, 11]. This assumption allows for a linear curve fit to the calibration data as shown in Fig. 3. The  $R^2$  coefficient is



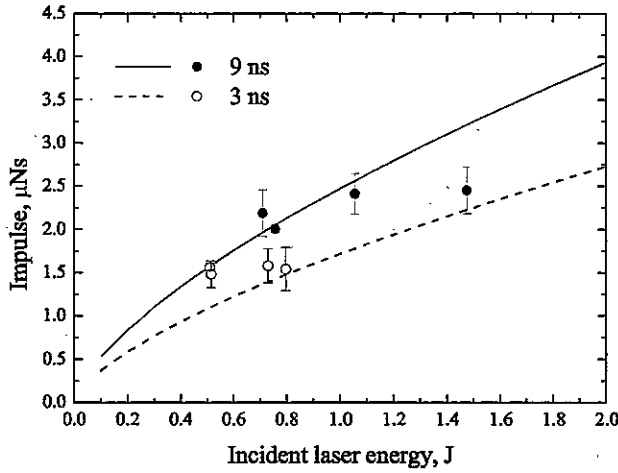


FIG. 4. Impulses measured on the shielded thrust stand as a function of incident laser energies for pulse duration of 3 ns and 9 ns.

determined to be 0.99922. The experimental data are converted into an impulse force using the conversion factor  $70 \mu\text{Ns}/\text{V}$  found from the calibration.

Figure 4 shows the impulses measured on the shielded thrust stand as a function of incident laser energies. The two data sets show the measured impulses for single laser pulse shot with pulse duration of 9 ns and 3 ns, respectively. Every data point plotted is the average result over more than three shots; the error is estimated for the associated standard deviation. In every shot, the incident laser energy and pulse duration have some error from the setting value. The effects of them are the main cause of the error bars on the measured impulse. When a non-magnetized iron cylinder is installed instead of permanent magnets, the measured impulse is zero. The result shows the interaction between the diamagnetic current in the laser-produced plasma and the magnetic field from the permanent magnets. Thus, the magnetic thrust chamber system for LFR is demonstrated to produce impulse experimentally.

The impulse is  $2.0 \mu\text{Ns}$  at the laser pulse duration of 9 ns, and it is  $1.5 \mu\text{Ns}$  at the laser pulse duration of 3 ns, when the incident laser energy is  $0.7 \sim 0.8 \text{ J}$ . The difference between 9 ns and 3 ns can be explained as follows. The lines shown in Fig. 4 represent the estimated impulse curves under the assumption that the impulse is the product of the plasma ablation mass and the ion acoustic speed, i.e.,  $S\tau\dot{m}C_s$ . All the plasma is assumed to be pushed back by the magnetic field before colliding the plate.  $S$  means the plasma ablation area of target assumed to be the surface of target where the solid angle is  $0.4\pi$ , as shown in Fig. 2. Thus,  $S$  is fixed to be  $7.9$

$\times 10^{-8} \text{ m}^2$ .  $\tau$  is the laser pulse duration. The solid and dashed lines are shown for pulse duration of 9 ns and 3 ns, respectively. The theoretical values are qualitatively corresponding to the experimental values as shown in Fig. 4. The plasma ablation mass per unit area per unit time,  $\dot{m}$  and the ion acoustic speed  $C_s$  are estimated as follows. The plasma expansion velocity into a vacuum is approximately equal to the ion acoustic speed [12].

$$\dot{m} = \frac{n_c^{2/3}}{Z} \left( \frac{3\eta_a I}{4f} \right)^{1/3} \sqrt{(1+Z)m_e^{1/3} m_i} \quad (1)$$

$$C_s = \left( \frac{3\eta_a I}{4fn_c} \right)^{1/3} \sqrt{\frac{(1+Z)m_e^{1/3}}{m_i}} \quad (2)$$

Equation (1) [12] gives  $\dot{m}$ , where  $m_e$  is the electron mass, and  $m_i$  is the ion mass. In this experiment, the laser cutoff density  $n_c$  is  $9.8 \times 10^{26} \text{ m}^{-3}$ , the charge number of ion  $Z$  is 4 ( $\text{C}^{4+}$  is assumed to be the primary ion in the plasma), the laser absorption rate  $\eta_a$  is assumed to be 1, the coefficient  $f$  is 0.08. Equation (2) [12] gives  $C_s$ .  $I$  is the incident laser intensity, which has the relationship  $I = E_L/S\tau$ , where  $E_L$  is the incident laser energy. According to these equations, the plasma ablation mass and expansion velocity increase with increasing incident laser intensity, that is,  $\dot{m} \propto I^{1/3}$  and  $C_s \propto I^{1/3}$ . When  $E_L$  is constant ( $\tau \propto I^{-1}$ ), the impulse is proportional to  $\tau\dot{m}C_s \propto I^{-1/3}$ , that is,  $\tau^{1/3}$ . Thus, the impulse increases theoretically with the laser pulse duration.

In the present experiments, the impulse on a magnetic thrust chamber system for LFR is measured directly by means of a pendulum thrust stand. Thus, the system is demonstrated experimentally for eventual use in a space propulsion system. It was also found that the impulse increases, as the laser pulse duration becomes longer. The measured impulse data are in good agreement with the impulses expressed theoretically as a product of the plasma ablation mass and the ion acoustic speed. The data obtained in these experiments will be useful for further investigating the mechanism of producing an impulse in a magnetic thrust chamber system for LFR.

#### ACKNOWLEDGMENTS

The authors wish to thank the Grant-in-Aid for Scientific Research (B), No. 21360418, and the Grant-in-Aid for JSPS Fellows sponsored by the Japan Society for the Promotion of Science, No. 22-1672, Japan. This work was performed under Collaborative Research, Institute of Laser Engineering, *Osaka University*, No. B1-19, 2009. We express our gratitude to Mr. Eiji Sato at *Osaka University* for helpful assistance.

[1] R. A. Hyde, L. L. Wood, and J. H. Nuckolls: AIAA Paper, 72 (1972), p. 1063.

[2] R. A. Hyde: Lawrence Berkeley Laboratory UCRL-88857

- (1983).
- [3] C. D. Orth, G. Klein, J. Sercel, N. Hoffman, K. Murray, and F. Chang-Diaz: Lawrence Livermore National Laboratory UCRL-96832 (1987).
  - [4] C. D. Orth: Lawrence Livermore National Laboratory UCRL-LR-110500 (2003).
  - [5] S. Uchida: *J. Plasma Fusion Res.*, **81** (2005), p. 186 [in Japanese].
  - [6] S. Uchida: *J. Plasma Fusion Res.*, **83** (2007), p. 271 [in Japanese].
  - [7] Y. Nagamine, and H. Nakashima: *Fusion Technology*, **35** (1999), p. 62.
  - [8] R. Kawabuchi, N. Matsuda, Y. Kajimura, H. Nakashima, and Y. P. Zakharov: *J. Phys. Conf. Ser.* **112** (2008), 042082.
  - [9] K. V. Vchivokv, H. Nakashima, Y. P. Zakharov, T. Esaki, T. Kawano, and T. Muranaka: *Jpn. J. Appl. Phys.* **42** (2003), p. 6590.
  - [10] H. Koizumi, A. Kakami, K. Komurasaki, and Y. Arakawa: *J. Jpn. Soc. Aeronaut. Space Sci.*, **51** (2003), p. 270 [in Japanese].
  - [11] H. Koizumi, K. Komurasaki, Y. Arakawa: *Rev. Sci. Instrum.*, **75** (2004), p. 3185.
  - [12] H. Azechi: *J. Plasma Fusion Res.*, **81** (2007), p. 2 [in Japanese].